Disposition of Calcium Release Units in Agarose Gel for an Optimal Propagation of Ca^{2+} Signals

Manfred H. P. Wussling,* Ines Aurich,* Oliver Knauf,* Helmut Podhaisky,† and Hans-Jürgen Holzhausen‡
*Julius Bernstein Institute of Physiology; †Institute of Numerical Mathematics; and ‡Institute of Pathology, Martin Luther University, Halle-Wittenberg, Germany

ABSTRACT Clusters of calcium-loaded sarcoplasmic reticulum (SR) vesicles in agarose gel were previously shown to behave as an excitable medium that propagates calcium waves. In a 3D-hexagonal disposition, the distance between neighboring spheres (which may stand for SR vesicles) is constant and the relationship between distance and vesicular protein concentration is expected to be nonlinear. To obtain a distribution of SR vesicles at different protein concentrations as homogeneous as possible, liquid agarose gels were carefully stirred. Electron micrographs, however, did not confirm the expected relationship between inter-SR vesicle distance and vesicular protein concentration. Light micrographs, to the contrary, resulted in a protein concentration-dependent disposition of clusters of SR vesicles, which is described by a linear function. Stable calcium waves in agarose gel occurred at SR vesicle protein concentrations between 7 and 16 g/l. At lower protein concentrations, local calcium oscillations or abortive waves were observed. The velocities of calcium waves were optimum at ~12 g/l and amounted to nearly 60 μm/s. The corresponding distance of neighboring calcium release units was calculated to be ~4 μm. The results further show that calcium signaling in the described reaction-diffusion system is optimal in a relatively small range of diffusion lengths. A change by ± 2 μm resulted in a reduction of the propagation velocity by 40%. It would appear that 1), the distance between calcium release units (clusters of ryanodine receptors in cells) is a sensitive parameter concerning propagation of Ca^{2+} signals; and 2), a dysfunction of the reaction-diffusion system in living cells, however, might have a negative effect on the spreading of intracellular calcium signals, thus on the cell's function.

INTRODUCTION

Numerous cellular processes are controlled by calcium that is stored mainly in the endoplasmic/sarcoplasmic reticulum (ER/SR), an intracellular organelle with distinct calcium ''sources'' and ''sinks''. Once released, cytosolic calcium ions diffuse from points of locally increased concentration to neighboring ER/SR ''sources'' (calcium channels) and induce further calcium release, termed ''calcium-induced calcium release'' (CICR). Subsequently, free calcium is sequestered by pumps located in the membranes of the ER/SR and the plasmalemma (Clapham, 1995). Concomitantly with such processes, calcium oscillations and/or calcium waves may occur (Wier et al., 1987; Wier and Blatter, 1991; Lipp and Niggli, 1993; Trafford et al., 1995; Clapham and Sneyd, 1995; Wussling and Salz, 1996; Ishida et al., 1999; Subramanian et al., 2001; Sell et al., 2002; Worth et al., 2003). The calcium wavespeed in cells of several species and at different temperatures has been observed to vary between 3 and 160 μm/s (Jaffe, 1993, 2002). Calcium waves in fertilizing eggs of *Xenopus laevis*, for instance, propagate with 20 μm/s (Camacho and Lechleiter, 1993). In neuronal cells of mammals, to the contrary, calcium waves travel with velocities beyond 100 μm/s, e.g., 160 μm/s in retinal cells of newborn ferrets (Stellwagen et al., 1999). Under the condition of calcium overload, in adult as well as embryonic stem cell-derived cardiac myocytes, spontaneous calcium waves may easily develop (Cheng et al., 1993; Haberland et al., 2000). They show steep increase and flat decay of the fluorescence intensity, propagate within 80–100 μm/s, and annihilate one another after collision due to refractoriness (Ishide et al., 1990; Wussling et al., 1997).

A presupposition for the development of spatiotemporal calcium patterns is not the integrity of a living cell but the presence of a reaction-diffusion system. The latter is given already when vesicles of the SR are embedded homogeneously or inhomogeneously in agarose gel with a composition similar to that of the cytosol. In such a system, with an apparent calcium diffusion coefficient of 215 μm^2/s (gel with SR vesicles) or 150 μm^2/s (gel with SR vesicles and mitochondria), calcium waves propagate with velocities of ~40 μm/s or even more (Wussling et al., 1999, 2001). Isolated mitochondria were previously shown to be excitable organelles that can generate travelling depolarization and Ca^{2+} waves (Ichas et al., 1997). Whereas energized mitochondria accelerate calcium waves in clustered SR vesicles, thapsigargin, a specific inhibitor of the SR calcium pump (SR CaATPase), slows down the wavespeed (Wussling et al., 1999). Spatiotemporal calcium patterns in gels with isolated cell organelles underlie, similar to living cells, the general principles of self-organization in excitable media, which numerically can be simulated by a reaction-diffusion model (Podhaisky and Wussling, 2004). This model predicts a biphasic dependence of the calcium wavespeed on the

Submitted October 7, 2003, and accepted for publication September 7, 2004.

Address reprint requests to Professor Manfred H. P. Wussling, Martin Luther University, Julius Bernstein Institute of Physiology, Halle-Wittenberg, Magdeburger Strasse 6, D-06097 Halle/S, Germany. Tel.: 49-345-557-1392; E-mail: manfred.wussling@medizin.uni-halle.de.

0006-3495/04/12/4333/10 $2.00

doi: 10.1529/biophysj.103.035089

distance between neighboring calcium release units. However, there are no corresponding experimental data yet.

In twitch fibers of frog skeletal muscle, calcium waves are reported to be involved in the excitation-contraction coupling including junctional and parajunctional clusters of ryanodine receptors (Zhou et al., 2003; Felder and Franzini-Armstrong, 2002). Calcium waves have been shown to play an important role in the normal physiological function of cardiac atrial myocytes, pacemaker cells, and Purkinje cells (Blatter et al., 2003). Cardiac atrial cells lack transverse tubuli (invaginations of the sarcolemma), so that calcium waves must spread over relatively long distances (Hüser et al., 1996). It may be supposed that in such cells, the distance between neighboring calcium release units critically influences the reaction-diffusion mechanism. In cat atrial cells, for instance, clusters of ryanodine receptors were found to be regularly disposed in the membranes of the SR with an average neighboring distance of ~ 2 μm, similar to a 3D lattice (Kockskämper et al., 2001). An activation of subsarcolemmal junctional Ca^{2+} release sites, usually initiated by an action potential, results in a significant increase of the cytosolic calcium concentration in the periphery of the cell and subsequent spreading of a calcium wave to the central nonjunctional SR in a regenerative fashion (CICR) with an unusually high propagation velocity of ~ 250 μm/s (Sheehan and Blatter, 2003). On the other hand, Ca^{2+} alternans-induced calcium waves have been shown to cause the development of atrial arrhythmias (Kockskämper and Blatter, 2002). Whatever the contribution of calcium waves to the cell's physiological or pathophysiological function is, the question arises, how does the distance of neighboring calcium release sites influence the mechanism of CICR?

In gels with homogeneously distributed SR vesicles, wave patterns depend on several parameters, e.g., total calcium concentration within the gel (Krannich, 2001). This work is aimed to systematically investigate 1), the range of the gel's SR vesicle protein concentration where calcium waves occur; 2), the relationship between the gel's SR vesicle protein concentration and the average distance between neighboring calcium release units; and 3), the dependence of the propagation velocity of calcium waves on that distance. One may expect, of course, that gel preparations with a SR vesicle protein concentration below a threshold do not propagate calcium waves. In other words, gel preparations are expected to be nonexcitable when the distance between neighboring calcium release units exceeds a critical value.

METHODS

SR vesicles

SR vesicles were prepared from the sarcoplasmic reticulum of skeletal muscles (*Longissimus dorsi*) of German landrace pigs according to a procedure described previously (Mickelson et al., 1986). The protein content of the SR vesicles which were stored at -80°C in a suspension containing 300 mM sucrose and 10 mM PIPES amounted to 29.3 g/l (suspension A).

Agarose gel system

We exclusively used the type VII agarose gel (low gelling temperature, Sigma, Heidelberg, Germany) and reagents of the purest grade commercially available. Agarose gel was dissolved in aqua bidest at 100°C for 5 min and cooled to a temperature of 37°C. After being mixed with buffer solution and the calcium indicator Fluo-4, a certain volume of the gel was transferred to an adequate volume of suspension A (SR vesicles) and stirred repeatedly to obtain SR vesicles homogeneously distributed in the agarose gel system (suspension B). Due to the replacement of SR vesicles by agarose gel, the total volume of suspension B was constant in all experiments and amounted to 24.7 μl, independent of the requested protein concentration. Suspension B was prepared immediately before each experiment. The composition of the final agarose gel system was (in mM) KCl 100, $MgCl_2$ 5, Na_2ATP 4, phosphocreatine 10, EGTA 0.04, Pipes 20, and $CaCl_2$ 0.025. . . .0.41 (dependent on SR vesicle protein concentration), Fluo-4 10, and 0.4% agarose gel. A set of four specimens (~ 6 μl each) derived from suspension B was stored in darkness in humid chambers until needed for the investigation with the confocal laser scanning microscope at room temperature. The duration of measurement was restricted by the consistency of the agarose gel. Increasing protein concentrations resulted in a more rapid solidifying of the gel and an impairment of the reproducibility of repetitive calcium waves. Good patterns were usually observed in fresh preparations during the first 20 min.

To reach a nearly constant calcium loading of the SR vesicles in the agarose gel system, it was important to keep constant the ratio of protein concentration and total calcium concentration in suspension B. Most of the calcium is stored in the SR vesicles. Therefore, $c_{Ca\text{-}tot} \approx c_{Ca\text{-}ves} V_A/V_B$, where $c_{Ca\text{-}tot}$ is the total calcium concentration, $c_{Ca\text{-}ves}$ is the vesicular calcium concentration, V_A is the volume of suspension A, and V_B is the volume of suspension B (24.7 μl in all experiments). On the other hand, $c_{Ca\text{-}tot} = k \times c_{Prot}$, where c_{Prot} is the protein concentration and k is the constant. In our experiments, a proportional factor of $k = 0.0253$ mmol/g proved to be optimal (Krannich, 2001). The background Ca^{2+} in gels with varying protein concentrations was measured initially and found to be constant in the order of magnitude of 10^{-8} M (Krannich, 2001).

Confocal laser scanning microsopy and data processing

For the measurements, a confocal laser scanning microscope (INSIGHT-PLUS, Meridian Instruments, Okemos, MI) with the Brakenhoff scan system, enabling a 100/s sample rate, was used (images of 512 $\times$ 480 pixels). Due to the use of a CCD camera (CCD 72 cooled by two Peltier batteries; Dage-MTI, Michigan City, IN), the frequency of captured frames actually amounted to 25 Hz. The computer-controlled Z-drive accessory provided optical sectioning with a step size of 0.6 μm at minimum. All frames obtained with a LWD 40$\times$ and NA 0.55 objective (Olympus, Tokyo, Japan) were recorded on videotape. After digitization with a frame grabber board (QuickCapture 1.13, Data Translation, Marlboro, MA) data were processed using software for the Macintosh OS D2-9.1 and the Macintosh IIci computer (IPLab Spectrum QC, Signal Analytics, Vienna, VA; NIH Image 1.43, Microsoft, Redmond, WA).

Electron microscopy and data processing

Additional agarose gel preparations with SR vesicles of varying density (protein concentrations between 3 g/l and 16 g/l) were prepared, fixed

(glutaraldehyde), stained (osmiumtetroxide) and embedded in epoxy. A series of semithin slices (35 μm in thickness) was manufactured suitable for the check in a light microscope at relatively low magnification. To store selected samples on the hard drive of a IIci Macintosh computer, a CCD camera (C 3077) with control unit (C 2400), an additional controller (II), and the Argus-10 image processor (Hamamatsu, Bridgewater, NJ) was used. Ultrathin slices (55 nm in thickness) were investigated using a 50–80 kV electron microscope (EM 902 A, Zeiss, Oberkochen, Germany). We used a semiautomatic approach to analyze the images obtained from the microscope: first, for each photo we marked the midpoints of SR vesicles (electron micrographs) or of clusters of SR vesicles (light micrographs) on a transparency. In a second step, we scanned the slides and applied simple image detection to the high-contrast pictures. That procedure gave us a list of coordinates of the midpoints. Finally, the nearest neighboring distance in that list has been evaluated using MATHEMATICA (Wolfram Research, Champaign, IL). The number of vesicles inside the images varied from 161 to 807. For the determination of the areas of clusters of SR vesicles the freeware ImageJ was used (Image Processing and Analysis in Java, http://rsb.info.nih.gov./ij/).

RESULTS

Protein concentration-dependent calcium waves and oscillations in agarose gel

Clusters of calcium-loaded SR vesicles, embedded in agarose gel with a free calcium concentration of $\sim 5 \times 10^{-8}$ M (Krannich, 2001) were demonstrated to propagate calcium waves with a velocity of 40 μm/s in the absence and 60 μm/s in the presence of mitochondria (Wussling et al., 1999). Fig. 1 shows a sequence of four phases (*A–D*) of a stimulated calcium wave spreading through a clustered area of ~ 300 μm $\times$ 450 μm (see *outline*) in agarose gel with a vesicular protein concentration of 16.32 g/l and in the presence of mitochondria. The arrow in the left lower corner of each frame points to the edge of the gel. The time between sequential images amounted to 1 s and the wavespeed was 64 μm/s in average. Wavespeed is related to the direction of the spreading wave, i. e., orthogonally to the wavefront (cf. Fig. 3 in Wussling et al., 1999), and was determined from intensity profiles. Note that the wave's fluorescent intensity is relatively high so that the wavefront appears clearly visible. In an isotropic 3D medium, calcium waves are expected to occur as spherical waves (or circular waves in the confocal plane). Fig. 1 shows deviations from circular wavefronts. This is surely due to inhomogeneities concerning either the distribution of the SR vesicles or of the fluorescent calcium indicator, possibly both. The observed calcium waves, however, were found to be stable at relatively high protein concentration (e.g., 16.32 g/l). They appeared repetitively and spread throughout the cluster with nearly constant velocity within a few minutes (not shown in Fig. 1).

In the following, we consider calcium patterns of gels without mitochondria. To avoid the development of larger SR fragmental clusters at lower protein concentrations, we distributed the vesicles as homogeneously as possible (by repeated stirring). Fig. 2 shows a typical calcium wave pattern at the protein concentration of 10.86 g/l. Each of the four consecutive frames (*A–D*) shows the same spot of a gel,

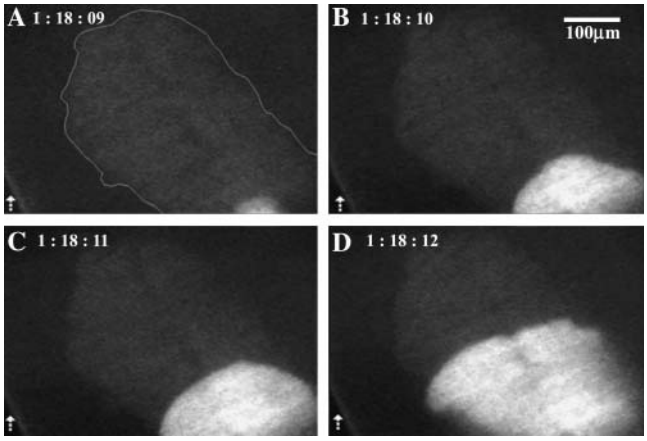

FIGURE 1 Propagating calcium wave in a cluster of SR vesicles and mitochondria in agarose gel with a SR vesicle protein concentration of 16.32 g/l (ratio of protein concentrations 5:1). Fluorescence is due to the presence of 10 μM of the calcium indicator Fluo-3 in the gel. Time between frames is 1 s (running time of the video recorder is displayed). In *A*, a stimulated wave becomes visible just on the bottom of the frame (stimulation by calcium ions). The cluster's edge is marked by an outline. For an estimate of the cluster's size, see calibration bar in frame *B*. (*B–D*) Spreading of the excitation (calcium wave) through the cluster with a speed of 64 μm on average. The relatively bright wave does not propagate with constant velocity in all directions. This is most likely due to inhomogeneities in the gel. Note the arrow in the lower left-hand corner of each frame which points to the edge of the gel.

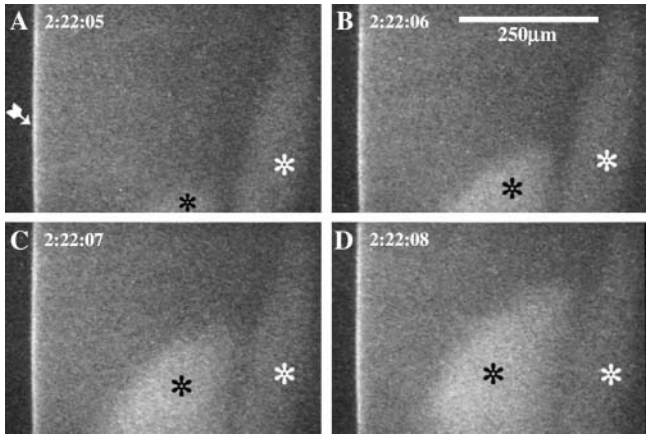

FIGURE 2 Propagation of a stimulated calcium wave in agarose gel with a SR vesicle protein concentration of 10.86 g/l (mitochondria not added). SR vesicles were homogeneously distributed in the gel, which contained 10 μM Fluo-4 as calcium indicator. (*A–D*) Time between sequential frames is 1 s (running time displayed). Note that 1), fluorescence intensity of the spreading wave (see *black asterisks*) is relatively low despite an enhanced sensitivity of Fluo-4 compared to Fluo-3; and 2), velocity of the spreading wave is relatively high (~ 70 μm/s) even in the absence of mitochondria. The excitable area by chance is restricted to an area between the edge of the gel (see *A*, *arrow* at left), which appears slightly curved due to the circularly shaped specimen, and an unexcitable region that acts as a wave barrier (see *white asterisk* on the right-hand side of each frame).

including its left slightly curved edge (see *arrow* in Fig. 2 *A*), at different times (see *insets*). To better visualize the spreading calcium wave, a black asterisk was stamped in the growing excitation area of each frame. White asterisks mark an unexcitable region that acts as a border for the spreading calcium wave. Note that the wave's brightness is relatively low so that the wavefront appears diffuse (in comparison to Fig. 1). Nonetheless, the wavespeed was higher at the SR protein concentration of 10.86 g/l in the absence, compared to the SR protein concentration of 16.32 g/l in the presence, of mitochondria (namely ~70 μm/s in Fig. 2 compared to 64 μm/s in Fig. 1). We later will show that the protein concentration of 11–12 g/l is optimal for propagating calcium waves in the agarose gel system.

It would appear that calcium waves do not propagate at protein concentrations below a critical level. Fig. 3, *A–P*, shows local calcium oscillations and a small movement of the wavefront toward the top of every frame (similar to an abortive wave) at the SR vesicle protein concentration of 1 g/l. The time between subsequent images is 1 s. Thus, Fig. 3 shows one full oscillation with a period of ~14 s (cf. frames *A* and *O* or *B* and *P*). A total of nine oscillations with a period of 15 ± 3.1 s (mean ± SD) were observed in the preparation corresponding to Fig. 3. Two points are worth mentioning:

1. At low SR vesicle density, visible calcium transients have been observed very seldom. Therefore, the frequency of such events with respect to the number of gel preparations and the selected areas within one preparation is difficult to quantify. The development of weak calcium oscillations or abortive waves is likely due to unavoidable inhomogeneities within the gel.
2. The fluorescence intensity in preparations with small SR vesicle protein concentrations was much lower than those with relatively high ones. To better demonstrate weak intensity fluctuations, we must apply arithmetic and filter operations. Each image of Fig. 3 was obtained by the image arithmetic operation $X + X - Y$ (using IPLab Spectrum QC), where X means any original image with a barely visible calcium signal and Y denotes background, i. e., the image before the development of a weak calcium signal. Frame M of Fig. 3 is considered to be background for the subsequent patterns. Frame P, for instance, resulted from the corresponding original image, X_P, by the operation $X_P + X_P - Y_M$, where $Y_M = M$. To further improve the contrast, we used pseudocolor and the filter function ''dilate'' (IPLab Spectrum QC).

Local and global distribution of SR vesicles

To reveal the dependence of the propagation velocity of calcium waves on the distribution of SR vesicles in the gel, we investigated electron micrographs of gels with protein concentrations varying between $c = 3$ g/l and $c = 16$ g/l and determined the mean inter-SR vesicle distance, d, as described above (Methods). The highest protein concentration in agarose gel was 16.32 g/l. Fig. 4 *A* shows a representative ultrathin slice (55 nm in thickness) of SR vesicles in agarose gel at $c = 9$ g/l. The mean inter-SR vesicle distance was $d = 193 \pm 53$ nm (mean ± SD; $n = 100$). The microsome's mean diameter resulted in $\Phi = 172 \pm 37$ nm (mean ± SD; $n = 100$ vesicles). The points shown in Fig. 4 *B* mark the SR

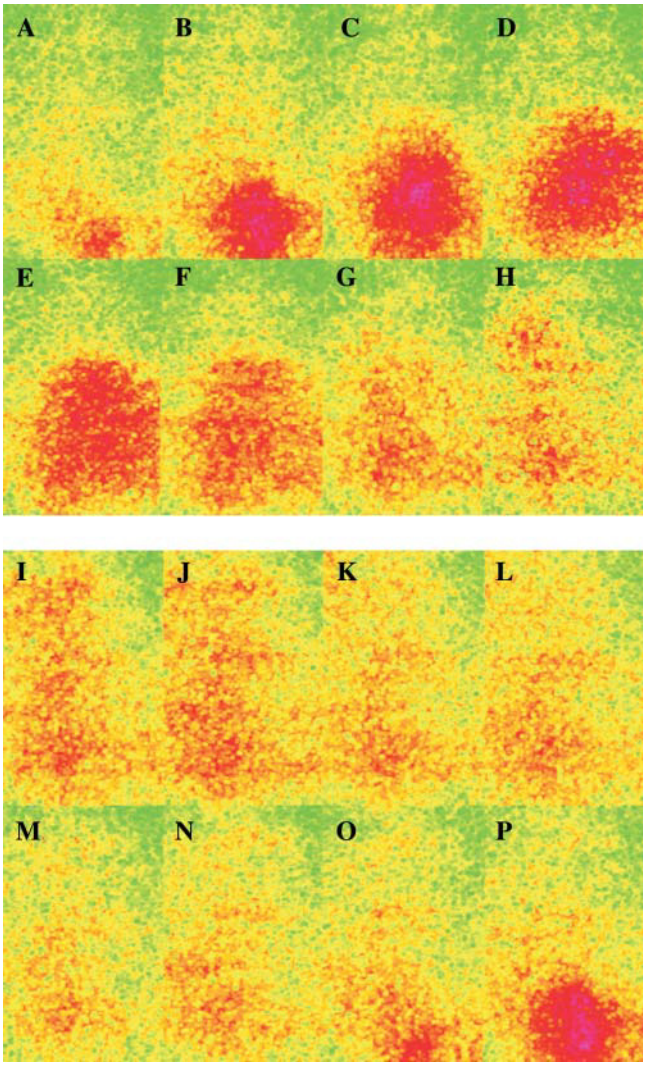

FIGURE 3 (*A–P*) Local calcium oscillations with a little upward shift of the excitation center in agarose gel with a very low SR vesicle protein concentration (1 g/l) and a Fluo-4 concentration of 10 μM. The time between sequential images (320 × 480 pixels or 237 × 356 μm each) is 1 s. One oscillation takes ~14 s (cf. frames *A* and *O* or *B* and *P*). Nine oscillations with a period of 15 ± 3.1 s (mean ± SD) were observed in this preparation (not shown). Fluorescence intensity was very weak at low SR vesicle protein concentrations. Software IPLab Spectrum QC arithmetic ($X + X - Y$) and filter (''dilate'') operations were applied to better demonstrate fluorescence fluctuations. Frame M is considered as background, so that frame P, for instance, results from $X_P + X_P - Y_M$ with $Y_M = M$. Frames are depicted in pseudocolor to further improve the visualizing of the weak fluorescence signals.

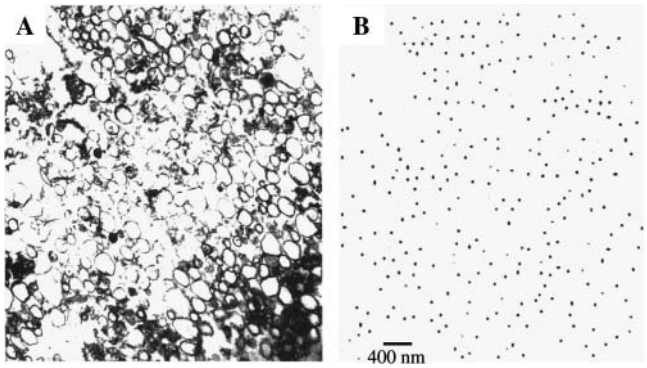

FIGURE 4 Scanned picture of a representative electron micrograph of SR vesicles in agarose gel (*A*). Thickness of the slice, 55 nm. SR vesicle protein concentration in gel, 16.32 g/l. This is the maximum in our experiments. Morphometric data: SR vesicle diameter, $\Phi = 172 \pm 37$ nm (mean ± SD; $n = 100$); center-to-center distance, $d = 193 \pm 53$ nm (mean ± SD; $n = 100$). (*B*) Dots correspond to the centers of the SR vesicles and have been depicted by hand. To determine the mean inter-SR vesicle distance, an objective procedure was applied (see Methods). Calibration bar is valid for both *A* and *B*.

vesicle's centers, which were used for the determination of the mean inter-SR vesicle distance.

Assuming a 3D-hexagonal disposition of spheres of the same size, the distance between the centers of neighboring spheres, d, is constant. Fig. 5 *A* schematically shows a 2D arrangement of hexagonal dense spheres with $d = d_A$ (see *bar*). A smaller concentration of spheres is expected to result in a greater distance between them. This is shown in Fig. 5 *B*, where $d = d_B = 2d_A$ (see *bar*). If $d \sim (1/c)^{1/3}$, then

$$d_B = d_A(c_A/c_B)^{1/3}. \quad (1)$$

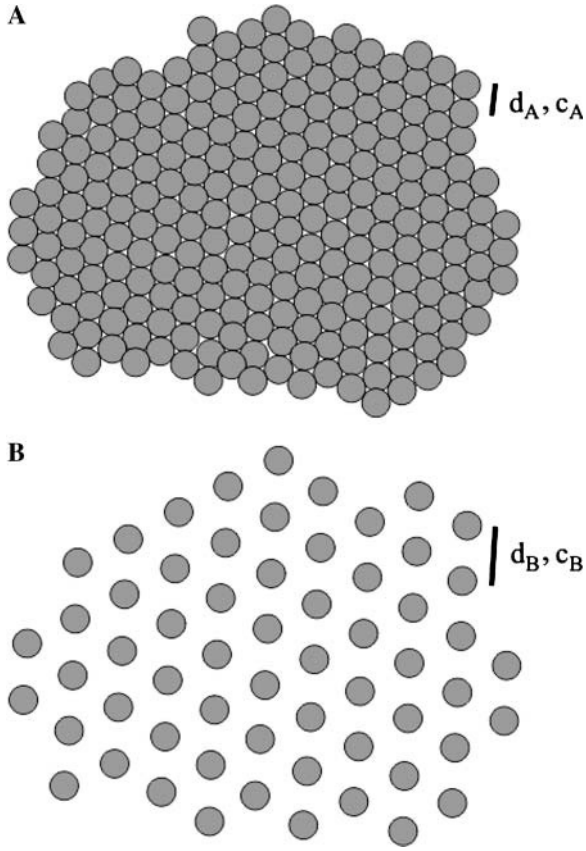

FIGURE 5 (*A*) Schematic layer of a hexagonal dense arrangement of spheres (which are assumed to represent SR vesicles). Center-to-center distance between neighboring spheres (see *bar*) corresponds to the sphere's diameter. (*B*) Schematic layer of the hexagonal arrangement after reduction of the number of spheres to one-eighth that of the upper arrangement. Center-to-center distance between neighboring spheres increased to twice that of the hexagonal dense arrangement (see *bar*): $d_B = 2d_A$. Abbreviations: *d*, intersphere distance; *c*, concentration.

The relationship between both inter-SR vesicle distance and protein concentration is also expected to obey Eq. 1. Surprisingly, our expectations have not been fulfilled, as shown in Fig. 6. The circles (mean ± SD, numbers in parentheses underneath = number of preparations) represent measured data (cf. *exp*.) fitted by a spline function. The thick-lined curve in Fig. 6 results from Eq. 1 (cf. *theor*.), where d_A and c_A, respectively, refer to the most right point (cf. *A*). In the case of globally homogeneously distributed SR vesicles, all points of Fig. 6 should be located on the calculated curve (cf. *theor*.). It is clearly shown that the SR vesicles are not distributed in the expected manner (Eq. 1) but locally clustered, independent of the gel's global protein concentration.

Let us turn to the global distribution of SR vesicles. Fig. 7 shows a light micrograph of clusters of SR vesicles with a protein concentration of 7 g/l in the gel at relatively small magnification (*calibration bar*, 100 μm). The clusters embedded in semithin slices (of 0.35 μm in thickness) were different in size. To determine the distances between neighboring clusters, the position of each cluster was marked in a central point by hand (not shown) analog to the marking of SR vesicles (see Fig. 4 *B*). The mean distance was obtained using the same procedure as for the determination of the inter-SR vesicle distance (see Methods). Fig. 8 shows the data at different protein concentrations (analog to that of Fig. 6). Circles (mean ± SD; numbers in parentheses underneath are the number of preparations) represent measured data and were fitted by a linear regression line. Due to the high density at protein concentrations >9 g/l, clusters of SR vesicles were difficult or impossible to distinguish. In the case of a protein concentration of 16 g/l with practically all clusters fusioned, we used the mean inter-SR vesicle distance as determined by electron microscopy (see Fig. 8, rightmost point, *A*, which corresponds to that of Fig. 6). Whereas the mean distance between neighboring clusters clearly decreases, the cluster's size was found to

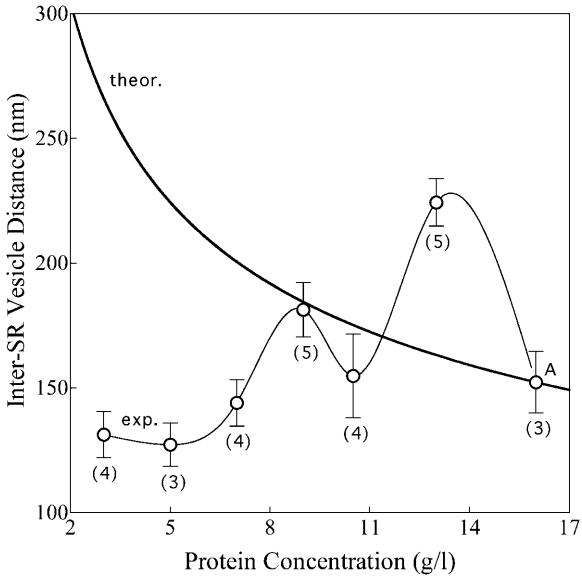

FIGURE 6 Inter-SR vesicle distance versus protein concentration. Experimental data are mean ± SD; number of gel preparations (electron micrographs) in parentheses underneath. Circles fitted by spline function. Circle *A* (*rightmost circle*) results from a protein concentration which was maximum in our experiments (16 g/l, in a few experiments 16.32 g/l). Thick line (*theor.*) according to Eq. 1: $d_B = d_A(c_A/c_B)^{1/3}$, where $c_A = 16$ g/l (see text). Note that the SR vesicles are not distributed as described by Eq. 1.

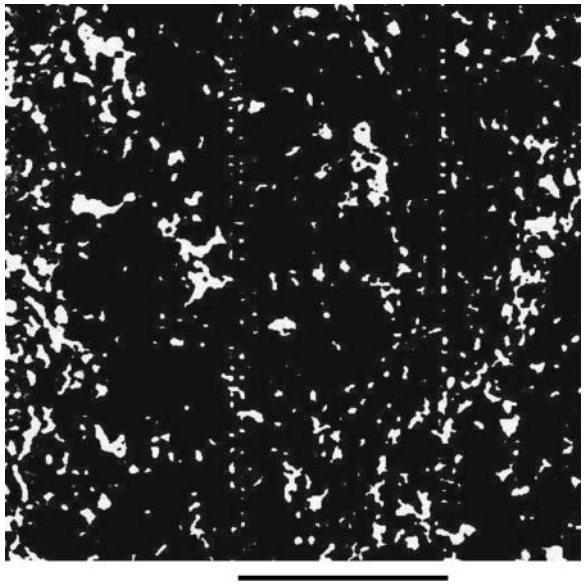

FIGURE 7 Light micrograph of clusters of SR vesicles at relatively small magnification (calibration bar, 100 μm). Protein concentration, 7 g/l gel. The clusters are embedded in semithin slices of 0.35 μm in thickness. The position of each cluster was marked by a central point (not shown) independent of the cluster's size. Some dots are artifacts due to the procedure of cutting of the preparation (see *orthogonal dotted stripes* starting close to the ends of the calibration bar) and were excluded from the analysis.

slightly increase from 18 to ~25 μm^2 within the corresponding range of protein concentrations (see *inset* of Fig. 8; data are mean ± SD, number in parentheses underneath are the number of preparations).

Influence of relative inter-SR vesicle distance on calcium wave propagation

To describe how distances of neighboring clusters or SR vesicles influence the propagation of calcium waves, wavespeeds were determined. Fig. 9 *A* shows propagation velocity in dependence on the protein concentration. Points are mean ± SD with numbers in parentheses indicating the number of investigated preparations. Protein concentrations of <7 g/l were found to generate abortive calcium waves in a relatively small region (~30 μm in diameter) or rather local oscillations than waves (cf. Fig. 3). Corresponding data (within outline in Fig. 9 *A*) are different from those of stable calcium waves which propagate throughout a relatively large area (a few hundreds of μm in distance; see Fig. 1). Therefore, we exclude the calcium signals which were (occasionally) detected at protein concentrations <7 g/l. At protein concentrations between 7 and 16.32 g/l stable calcium waves with velocities between 28 and 63 μm/s were observed. The velocity was maximum at ~12 g/l (see *asterisk*). The decrease of the wavespeed beyond the protein concentration of 12 g/l was originally unexpected (i.e., before corresponding model simulations). We supposed that shorter diffusion distances improved the generation and propagation of calcium waves. Though, as later shown, the decay of wavespeed at higher protein concentrations (i.e., shorter distances between neighboring clusters of SR vesicles) is possibly due to a prevailing effect of calcium pumps (SR Ca-ATPases). Fig. 9 *B* shows propagation velocity relative to the maximum, marked by an asterisk (see Fig. 9 *A*), in dependence on the mean distance between neighboring SR vesicle clusters. Estimates of distances were based on the data shown in Fig. 8 (*regression line*). Note that the points of Fig. 9 *B* (means ± SD) correspond to those of Fig. 9 *A* with the exception of the data within the outlined area. Fig. 9 *B* shows that the calcium signaling seems to be optimal in a relatively small range of distance. A deviation of ±2 μm (see *horizontal dashed line* in Fig. 9 *B*) from the optimal distance of ~4 μm (i.e., where wavespeed is maximum) results in a reduction of the propagation velocity by 40% (see *vertical dashed line* in Fig. 9 *B*).

DISCUSSION

Calcium waves and oscillations

Calcium is involved in numerous intra- and intercellular pathways that control the function of living cells (Berridge, 1993, 1997). This ubiquitous element undergoes spatial and temporal transients of cytosolic concentration both in periodically active cells (e.g., cardiocytes) and in those responding to random stimuli (e.g., cochlear hair cells,

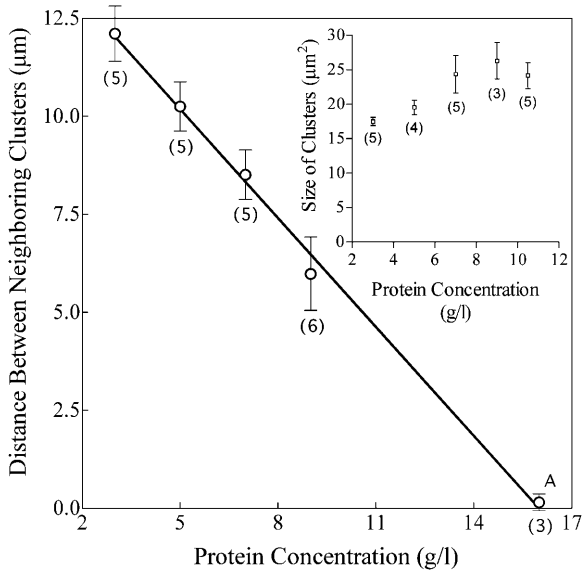

FIGURE 8 Distance between neighboring clusters (Y) versus protein concentration (X). Experimental data are mean ± SD, with numbers of preparations (light micrographs) in parentheses underneath. Linear regression line, $Y = -0.9261 \times X + 14.81$; $r^2 = 0.9964$. Due to the high density of clusters at protein concentrations above 9 g/l, the determination of mean distances was impossible. Circle A, therefore, results from the analysis of electron micrographs and implies inter-SR vesicle distance. It is identical with the rightmost circle of Fig. 6, which was called A as well. Inset shows size of clusters versus protein concentration. Data are mean ± SD, with numbers of light micrographs in parentheses underneath.

fertilizing oocytes). In cardiac cells, calcium sparks are considered to be the origin of calcium waves (Cheng et al., 1993, 1996), which propagate due to regenerative calcium release (Wussling and Salz, 1996; Wussling et al., 1997). A model proposed by Izu et al. (2001) predicts the velocity of calcium waves in cardiac cells to depend on kinetic parameters (rate of Ca^{2+} release, total amount of Ca^{2+} released, Ca^{2+} sensitivity of calcium release units (CRUs)) and on the disposition of neighboring CRUs.

Disposition of CRUs in agarose gel

If SR vesicles (see electron micrograph, Fig. 4) are considered as spheres with a diameter of 172 ± 37 nm (mean ± SD), the microsomes' surface area is calculated to vary between 85,000 nm^2 and 205,000 nm^2. Based on morphometric data concerning CRUs of the junctional sarcoplasmic reticulum of skeletal muscle fibers (Franzini-Armstrong et al., 1999), the area of a cluster of functionally cooperating ryanodine receptors (RyRs) may be estimated. If the number of RyRs (feet) per CRU amounts to 30 ± 11 (mean ± SD, determined from the data of 11 skeletal muscle types according to Table 1 of Franzini-Armstrong et al., 1999) and the feet-to-feet distance is 29 nm, then an area of 17,000 nm^2. . . .36,000 nm^2 per CRU results. Thus, the number of CRUs per SR vesicle might vary between 2 (large area of CRU, small surface area of microsome) and 12 (small area of CRU, large surface area of microsome), theoretically. Unfortunately, we don't have corresponding immunofluorescence data. The SR vesicles that we used in the experiments described above stem from heavy protein fractions. It is assumed, therefore, that vesicles with at least one or rather more CRUs form the majority of the microsomes.

Clusters of SR vesicles and calcium signals in agarose gel

In gels, spontaneous or stimulated calcium waves were observed to propagate throughout clusters of SR vesicles (Wussling et al., 1999). To investigate how wave propagation depends on the disposition of neighboring CRUs, the protein concentration of SR vesicles was varied. The relationship between mean inter-SR vesicle distance and protein concentration was supposed to be nonlinear. Despite several efforts toward a homogeneous distribution similar to a lattice with hexagonal disposition of the microsomes (see Fig. 5), we failed to confirm the expected relationship (Fig. 6). Actually, SR vesicles appear homogeneously distributed within a single cluster, i.e., locally (Fig. 4) but not globally in the whole agarose gel. The light micrograph of Fig. 7 clearly shows SR vesicles distributed in clusters. This might be due to electrostatic forces that prevent the separation of the microsomes. Clusters of SR vesicles, to the contrary, were distributed nearly homogeneously with monotoneously decreasing center-to-center distance as SR vesicle protein concentration increases (Fig. 8). The inset of Fig. 8 shows an enhancement of the cluster's size with increasing protein concentration from 3 to 9 g/l. This might be due to electrostatic and/or unavoidable stirring effects. However, since the mean area of the clusters is not constant in the range of protein concentrations where clusters may be distinguished (see *inset* of Fig. 8), we cannot exclude a certain influence of its size on the mean distance of neighboring clusters. Supposing a constant cluster size, that distance is expected to decay with increasing protein concentration, too, but not basically differently than the regression line of Fig. 8 does. Since the SR vesicle cluster's size is relatively constant at protein concentrations >7 g/l, the optimum intercluster distance (see Fig. 9 *B*) is likely not too far from being exact.

At relatively small protein concentrations (e.g., 1 g/l) local calcium oscillations (occasionally abortive waves) instead of globally spreading calcium waves were observed (Fig. 3). Local oscillations may be considered as proof of the excitability of the reaction-diffusion system, at least of isles of the gel preparation (or clusters of SR vesicles) scanned confocally. At SR vesicle protein concentrations <7 g/l (i.e., center-to-center distance between neighboring calcium release sites >8.3 μm), however, stable calcium waves did not occur. The reason is that the distance between potential calcium ''sources'' (or the diffusion length between CRUs)

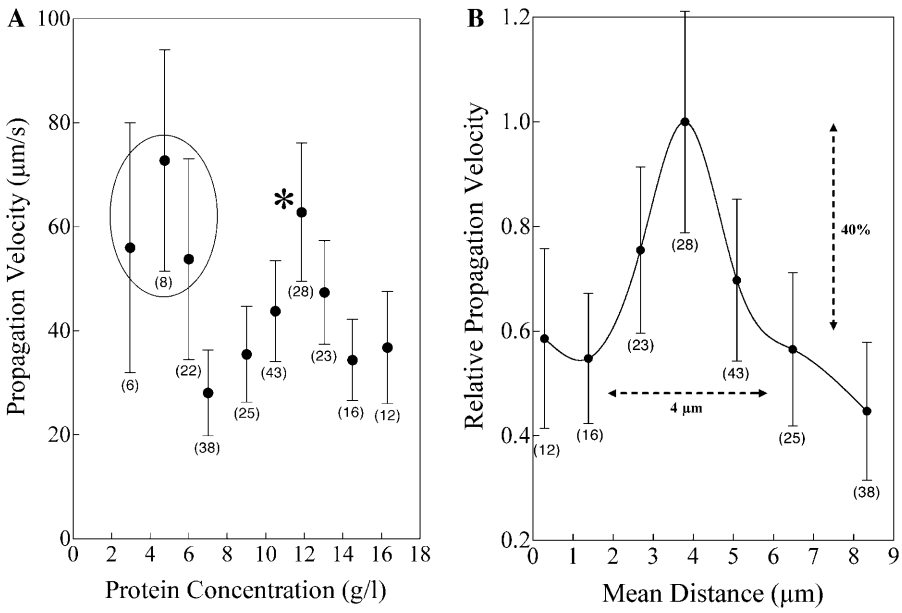

FIGURE 9 (*A*) Propagation velocity of calcium waves at different SR vesicle protein concentration. Data are mean ± SD, with number of preparations in parentheses underneath. At protein concentrations of <7 g/l, abortive calcium waves, or rather local oscillations than waves, were observed in relatively small regions (cf. Fig. 3). The data within the outline are different from those of stable calcium waves, which propagate throughout a relatively large area (a few hundreds of μm in diameter; see Fig. 1). Wavespeed appears to be optimal at a protein concentration of 11.86 g/l (see *asterisk*). (*B*) Relative propagation velocity versus mean distance as calculated from the curve fit of Fig. 8. Again, data are mean ± SD with number of preparations in parentheses underneath. The maximum corresponds to that point in *A* which is marked by an asterisk. Note that an increase as well as a decrease of the mean distance (between neighboring SR vesicle clusters), which relates to the maximum wavespeed, results in a considerable decrease of wavespeed. Wavespeed is maximum at a mean distance of 4 μm and decays by 40% (see *vertical dashed line*) when distance increases or decreases by 2 μm (see *horizontal dashed line*).

is too large to sustain the regenerative calcium release mechanism in the gel. The wavespeed was shown to be optimum at a protein concentration of 12 g/l or a center-to-center distance of nearly 4 μm and to significantly decay at smaller as well as greater distances between neighboring calcium ''sources'' (Fig. 9 *B*). This is an interesting result inasmuch as calcium ''sources'' and ''sinks'' would be expected to remain at a fixed ratio independent of the concentration of SR vesicles in the gel. According to Spiro and Othmer (1999), the calcium reuptake through pumps is considered to follow a Michaelis-Menten kinetics, i. e., the actual rate is a simple function of the local calcium concentration only. This is in contrast to the calcium release channels that are supposed to work autocatalytically and hence with a time delay. This can be modeled with an additional state variable describing the nonrefractory fraction of the channels and an additional ordinary differential equation for this state. Numerical calculations of a corresponding model basically resulted in biphasic characteristics of wavespeed versus the vesicle's density, as shown previously (Podhaisky and Wussling, 2004).

Comparison of gels with cells

In our artificial gel system we experimentally could vary the distance between clusters of CRUs. An optimum (with respect to the propagation velocity of calcium waves) of 4 μm is similar but not identical, with average distances between individual calcium release sites of living cells as reported previously (cardiac cells: Kockskämper et al., 2001; Sobie et al., 2002; *Xenopus* oocytes: Shuai and Jung, 2003). A quantitative comparison of the optimum intercluster distance of gels with living cells is a problem inasmuch as the function of calcium release sites and pumps in the membranes of SR vesicles embedded in agarose gel is likely impaired, in general, compared to the intact SR/ER of living cells. An impairment of the SR function, however, might require shorter distances between neighboring clusters of CRUs to enable regenerative calcium release. It should be emphasized that SR vesicles are the result of a stressful procedure that may interfere with distinct properties of the SR membranes. A second concern is that we embedded SR vesicles in an artificial gel with features that are similar to but not necessarily identical with the cytoplasm of living cells (Pollack, 2001). This opinion is supported by different apparent calcium diffusion coefficients measured by the same method both in cardiac myocytes (120 $\mu m^2/s$) and agarose gels with embedded SR vesicles (215 $\mu m^2/s$) (Wussling et al., 1997, 2001).

The calcium signaling is more stable and faster in the neighborhood of mitochondria (Hajnóczky et al., 2000). As previously shown, well-energized mitochondria accelerate the propagation of calcium waves in cells (Jouaville et al., 1995) and gels (Wussling et al., 1999) by ~50%, which is most likely due to the cooperation of both SR and mitochondria (Duchen, 1999). It would appear that an improvement of the SR vesicle's function, however, not only increases the velocity of spreading calcium waves but also may change the critical distance between neighboring clusters of CRUs. To avoid additional clustering, we did

not add mitochondria to the gels with embedded SR vesicles with the exception of only one preparation (see Fig. 1).

In summary, an artificial gel system which allows us to vary the distance between calcium ''sources'' on the one hand and calcium ''sinks,'' on the other hand, was investigated. We have shown that the disposition of calcium release units in agarose gels with embedded vesicles of the sarcoplasmic reticulum critically influences the regenerative mechanism of calcium release underlying the spreading of calcium waves. The relationship of mean distance between neighboring calcium release units (SR vesicles and clusters of SR vesicles) versus protein concentration was determined from electron micrographs and light micrographs using a home-made software (see Methods). The main result of the experiments is that stable calcium waves exclusively occurred in a range of the distance between either single SR vesicles or clusters of SR vesicles from nearly 200 nm to 8.3 μm. Calcium wavespeed peaked at a distance of 4 μm between neighboring clusters of SR vesicles. This qualitatively agrees with the reaction-diffusion model of Podhaisky and Wussling (2004). Because of the dependence of the calcium signaling on the inter-SR vesicle cluster distance within the artificial system presented here, we would think that a dysfunction of calcium ''sources'' and ''sinks'' in living cells, which is expected to increase the distance of neighboring release sites, however, might have a negative effect on the intracellular spreading of calcium signals, and thus on the cell's function.

We graciously thank Dr. Martina Paetzel, Cleveland, OH (and University of Halle/S, Germany), for helping us with the final draft of the manuscript and for her valuable comments and critique.

REFERENCES

Berridge, M. J. 1993. Inositol triphosphate and calcium signalling. *Nature*. 361:315–325.

Berridge, M. J. 1997. Elementary and global aspects of calcium signalling. *J. Physiol.* 499:291–306.

Blatter, L. A., J. Kockskämper, K. A. Sheehan, A. V. Zima, J. Hüser, and S. L. Lipsius. 2003. Local calcium gradients during excitation-contraction coupling and alternans in atrial myocytes. *J. Physiol.* 546:19–31.

Camacho, P., and J. D. Lechleiter. 1993. Increased frequency of calcium waves in *Xenopus laevis* oocytes that express a calcium ATPase. *Science*. 260:226–229.

Cheng, H., W. J. Lederer, and M. B. Cannell. 1993. Calcium sparks – elementary events underlying excitation-contraction coupling in heart muscle. *Science*. 262:740–744.

Cheng, H., M. R. Lederer, W. J. Lederer, and M. B. Cannell. 1996. Calcium sparks and $[Ca^{2+}]_i$ waves in cardiac myocytes. *Am. J. Physiol. Cell Physiol.* 270:C148–C159.

Clapham, D. E. 1995. Calcium signaling. *Cell.* 80:259–268.

Clapham, D. E., and J. Sneyd. 1995. Intracellular calcium waves. *In* Advances in Second Messengers and Phosphoprotein Research. A. R. Means, editor. Raven Press, New York. 1–24.

Duchen, M. R. 1999. Contributions of mitochondria to animal physiology: from homeostatic sensor to calcium signalling and cell death. *J. Physiol.* 516:1–17.

Felder, E., and C. Franzini-Armstrong. 2002. Type 3 ryanodine receptors of skeletal muscle are segregated in a parajunctional position. *Proc. Natl. Acad. Sci. USA*. 99:1695–1700.

Franzini-Armstrong, C., F. Protasi, and V. Ramesh. 1999. Shape, size, and distribution of Ca^{2+} release units in couplons in skeletal and cardiac muscles. *Biophys. J.* 77:1528–1539.

Haberland, A., M. Wilhelm, A. M. Wobus, and M. Wussling. 2000. Confocal calcium signals in cardiac myocytes derived from embryonic stem (ES) cells. *Pflügers Archiv, Eur. J. Physiol.* 439:R360.

Hajnóczky, G., G. Csordás, M. Madesh, and P. Pacher. 2000. The machinery of local Ca^{2+} signalling between sarcoendoplasmic reticulum and mitochondria. *J. Physiol.* 529:69–81.

Hüser, J., S. L. Lipsius, and L. A. Blatter. 1996. Calcium gradients during excitation-contraction coupling in cat atrial myocytes. *J. Physiol.* 494:641–651.

Ichas, F., L. S. Jouaville, and J. P. Mazat. 1997. Mitochondria are excitable organelles capable of generating and conveying electrical and calcium signals. *Cell.* 89:1145–1153.

Ishida, H., C. Genka, Y. Hirota, H. Nakazawa, and W. H. Barry. 1999. Formation of planar and spiral Ca^{2+} waves in isolated cardiac myocytes. *Biophys. J.* 77:2114–2122.

Ishide, N., T. Urayama, K. Inoue, T. Komaru, and T. Takishima. 1990. Propagation and collision characteristics of calcium waves in rat myocytes. *Am. J. Physiol.* 259:H940–H950.

Izu, L. T., W. G. Wier, and C. W. Balke. 2001. Evolution of cardiac calcium waves from stochastic calcium sparks. *Biophys. J.* 80: 103–120.

Jaffe, L. F. 1993. Classes and mechanisms of calcium waves. *Cell Calcium.* 14:738–745.

Jaffe, L. F. 2002. On the conservation of fast calcium wave speeds. *Cell Calcium.* 32:217–229.

Jouaville, L. S., F. Ichas, E. L. Holmuhamedov, P. Camacho, and J. D. Lechleiter. 1995. Synchronization of calcium waves by mitochondrial substrates in *Xenopus laevis* oocytes. *Nature*. 377:438–441.

Kockskämper, J. and L. A. Blatter. 2002. Subcellular Ca^{2+} alternans represents a novel mechanism for the generation of arrhythmogenic Ca^{2+} waves in cat atrial myocytes. *J. Physiol.* 545:65–79.

Kockskämper, J., K. A. Sheehan, D. J. Bare, S. L. Lipsius, G. A. Mignery, and L. A. Blatter. 2001. Activation and propagation of Ca^{2+} release during excitation-contraction coupling in atrial myocytes. *Biophys. J.* 81:2590–2605.

Krannich, K. 2001. Confocal calcium signals in an in vitro system with vesicles of the sarcoplasmic reticulum. PhD thesis. Martin Luther University, Halle-Wittenberg, Germany.

Lipp, P., and E. Niggli. 1993. Microscopic spiral waves reveal positive feedback in subcellullar calcium signaling. *Biophys. J.* 65:2272–2276.

Mickelson, J. R., J. A. Ross, B. K. Reed, and C. F. Louis. 1986. Enhanced Ca^{2+}-induced calcium release by isolated sarcoplasmic reticulum vesicles from malignant hyperthermia susceptible pig muscle. *Biochim. Biophys. Acta*. 862:318–328.

Podhaisky, H., and M. H. P. Wussling. 2004. The velocity of calcium waves is expected to depend non-monotoneously on the density of the calcium release units. *Mol. Cell. Biochem.* 256-257:387–390.

Pollack, G. H. 2001. Cells, Gels and the Engines of Life: A New, Unifying Approach to Cell Function. Ebner and Sons, Seattle, WA.

Sell, M., W. Boldt, and F. Markwardt. 2002. Desynchronising effect of the endothelium on intracellular Ca^{2+} concentration dynamics in vascular smooth muscle cells of rat mesenteric arteries. *Cell Calcium.* 32:105–120.

Sheehan, K. A., and L. A. Blatter. 2003. Regulation of junctional and non-junctional sarcoplasmic reticulum calcium release in excitation-contraction coupling in cat atrial myocytes. *J. Physiol.* 546:119–135.

Shuai, J. W., and P. Jung. 2003. Optimal ion channel clustering for intracellular calcium signaling. *Proc. Natl. Acad. Sci. USA*. 100:506–510.

Sobie, E. A., K. W. Dilly, J. dos Santos Cruz, W. J. Lederer, and M. S. Jafri. 2002. Termination of cardiac Ca^{2+} sparks: an investigative mathematical model of calcium-induced calcium release. *Biophys. J.* 83:59–78.

Spiro, P. A., and H. G. Othmer. 1999. The effect of heterogeneously-distributed RyR channels of calcium dynamics in cardiac myocytes. *Bull. Math. Biol.* 61:651–681.

Stellwagen, D., C. J. Shatz, and M. B. Feller. 1999. Dynamics of retinal waves are controlled by cyclic AMP. *Neuron.* 24:673–685.

Subramanian, S., S. Viatchenko-Karpinski, V. Lukyanenko, S. Györke, and T. Wiesner. 2001. Underlying mechanisms of symmetric calcium wave propagation in rat ventricular myocytes. *Biophys. J.* 80:1–11.

Trafford, A. W., P. Lipp, S. C. O'Neill, E. Niggli, and D. A. Eisner. 1995. Propagating calcium waves initiated by local caffeine application in rat ventricular myocytes. *J. Physiol.* 489:319–326.

Wier, W. G., and L. A. Blatter. 1991. Ca^{2+} oscillations and Ca^{2+} waves in mammalian cardiac and vascular smooth muscle cells. *Cell Calcium.* 12:241–254.

Wier, W. G., M. B. Cannell, J. R. Berlin, E. Marban, and W. J. Lederer. 1987. Cellular and subcellular heterogeneity of $[Ca^{2+}]_i$ in single heart cells revealed by fura-2. *Science.* 235:325–328.

Worth, R. G., M. K. Kim, A. L. Kindzelskii, H. R. Petty, and A. D. Schreiber. 2003. Signal sequence within FcγRIIA controls calcium wave propagation patterns: Apparent role in phagolysosome fusion. *Proc. Natl. Acad. Sci. USA.* 100:4533–4538.

Wussling, M. H. P., K. Krannich, V. Drygalla, and H. Podhaisky. 2001. Calcium waves in agarose gel with cell organelles: implications of the velocity curvature relationship. *Biophys. J.* 80:2658–2666.

Wussling, M. H. P., K. Krannich, G. Landgraf, A. Herrmann-Frank, D. Wiedenmann, F. N. Gellerich, and H. Podhaisky. 1999. Sarcoplasmic reticulum vesicles embedded in agarose gel exhibit propagating calcium waves. *FEBS Lett.* 463:103–109.

Wussling, M. H. P., and H. Salz. 1996. Nonlinear propagation of spherical calcium waves in rat cardiac myocytes. *Biophys. J.* 70:1144–1157.

Wussling, M. H. P., K. Scheufler, S. Schmerling, and V. Drygalla. 1997. Velocity-curvature relationship of colliding spherical calcium waves in rat cardiac myocytes. *Biophys. J.* 73:1232–1242.

Zhou, J., L. Csernoch, B. Launikonis, G. Brum, M. D. Stern, H. Cheng, and E. Rios. 2003. Concerted vs. sequentional openimg of vast arrays of channels in Ca^{2+} sparks of twitch muscle. *Biophys. J.* 84(Suppl.):9a.